catalysts

MDPI

Article

Fivefold Enhanced Photoelectrochemical Properties of ZnO Nanowire Arrays Modified with C_3N_4 Quantum Dots

Hao Yang [1], Zhiliang Jin [1,*], Hongyan Hu [2,*], Gongxuan Lu [2] and Yingpu Bi [2]

[1] School of Chemistry and Chemical Engineering, Beifang University of Nationalities, Yinchuan 750021, China; yhabc163@163.com

[2] State Key Laboratory for Oxo Synthesis and Selective Oxidation, Lanzhou Institute of Chemical Physics, Chinese Academy of Science, Lanzhou 730000, China; gxlu@lzb.ac.cn (G.L.); yingpubi@licp.ac.cn (Y.B.)

* Correspondence: zl-jin@nun.edu.cn (Z.J.); huhongyan@licp.cas.cn (H.H.); Tel.: +86-951-2067915 (Z.L.); +86-931-4968178 (H.H.)

Academic Editor: Vincenzo Baglio
Received: 17 December 2016; Accepted: 20 March 2017; Published: 24 March 2017

Abstract: A facile and effective growing strategy of graphite-like carbon nitride quantum dots (CNQDs) modified on ZnO nanowire array composite electrodes has been successfully designed and prepared for the first time. The remarkable quantum enhanced properties were carefully studied by means of scanning electron microscope (SEM), transmission electron microscopy (TEM), X-ray photoelectron spectroscope (XPS), UV-vis diffuse reflectance, PEC performance, and photocatalytic hydrogen production, and the results were in good agreement. Fivefold enhanced photoelectrochemical performances of this novel hierarchical hetero-array prepared in this paper compared with pure ZnO nanowire arrays were obtained under UV-light. The effect was attributed to the remarkable charge separation between CNQDs and ZnO nanowire arrays. Additional investigations revealed that the particular structure of CNQDs/ZnO composites contributed to the separation of a photon-generation carrier and an enhanced photoelectric current. Moreover, the absorption edge of CNQD-modified ZnO nanowire arrays was slightly broadened, and the diameter was reduced as well. The photoelectrochemistry hydrogen evolution splitting water using simulated solar irradiation exhibited the foreground of a possible application of a mechanism of photoelectrochemistry hydrogen evolution over CNQDs/ZnO composite electrodes.

Keywords: graphene-like C_3N_4; quantum dots; ZnO nanowire arrays; photoelectrochemical properties

1. Introduction

The growing environmental problems and energy crisis have been paid an increasing amount of attention. It is urgent to find a strategy with an efficient, clean, and low-cost alternative to traditional energy sources. Here, photoelectrochemical (PEC) water splitting was promising as a solution to resolve environmental problems and energy crises [1–3]. However, there is a challenge in developing a photoanode with high stability and efficiency due to the fact that most photoanode materials have a wide band gap and are a grave recombination of the electron-hole pairs [4–6]. Compared with other semiconductors such as single elements and sulfides, metal oxides have been widely concerned and studied because of their low cost and high stability. Among them, zinc oxide (ZnO) due to the low initial potential and the ability to quickly transfer electrons to stimulate more people to study it [7–9], Lei et al. synthesized ZnO quantum dots and was employed to enhance H_2 evolution for triazine imide and graphitic carbon nitride (g-C_3N_4) [10]. Moreover, Kang et al. demonstrated that coating nafion polymer films on the surface of ZnO thin photoanode exhibited photoelectric properties [11]. A zinc

oxide nanowire array with one-dimensional vertical growth, due to its excellent charge transfer and photocatalytic performance, has become a promising optoelectronic anode material [12,13]. However, the large band gap (3.37 eV) limits the utilization of ZnO nanowire arrays. Many efforts have been made to modify it to overcome these drawbacks, including element doping, other semiconductor composites, etc. [14–19].

Carbon nitrides (C_3N_4), especially g-C_3N_4, possess a very high thermal and chemical stability, namely, outstanding mechanical, electrical, thermal, and optical properties [20–23]. Quantum confinement occurs when the material sizes are less than 100 nm [24–27]. More recently, Yang and coworkers exhibited that the nitrogen-doped carbon quantum dots can improve the photocatalytic properties of CuO [28]. In addition, Chen et al. reported that the g-C_3N_4 quantum dots (CNQDs) modified TiO_2 and significantly enhanced photoelectric performance [29]. Thus, the design and construction of zero-dimensional (0D) quantum dots on ZnO nanowires are used to form strong quantum confinement, which is an effective means of enhancing photoelectric efficiency.

There has not yet been any report of 0D CNQDs applied to photoelectric spitting water. We successfully prepared a few layers of g-C_3N_4 nanosheets via a thermal condensation method suggested by Liu et al. [30,31]. g-C_3N_4 nanoribbons (CNNRs) were obtained by acidic etching g-C_3N_4 nanosheets, and CNQDs were then accomplished by pyrolysis CNNRs at 200 °C. A facile coating of ZnO@CNQD composite electrodes was prepared and the solar simulating irradiation-driven PEC efficiency of ZnO@CNQDs was greatly improved. Fivefold enhanced photoelectrochemical performances of this novel hierarchical hetero-array prepared in this paper, compared with the pure ZnO nanowire arrays, were obtained under UV-light, and a possible application foreground of photocatalytic water splitting for hydrogen production evolution was exhibited.

2. Results and Discussion

2.1. Morphology and Structure

Typical scanning electron microscopy imaging of ZnO nanowire arrays is shown in Figure 1A. It shows that ZnO nanowire arrays are uniformly grown in Fluorine-Tin Oxide (FTO) and that the average diameter of ZnO nanowire arrays is about 200 nm. From Figure 1B, we can calculate that the ZnO nanowires have vertical lengths of about 2 μm from the horizontal cross section graph. Here, we can clearly observe the vertically well-aligned ZnO nanowire arrays. The carbon nitride quantum dots with a diameter of about 20 nm on the surface of the ZnO nanowire arrays are shown in Figure 1C. Figure 1D gives the XRD patterns of the ZnO anneal and the ZnO@CNQDs-2, ZnO@CNQDs-4, and ZnO@CNQDs-6 composite photo-anodes samples. It clearly shows diffraction peaks, which are well indexed to ZnO (JCPDS 05-0664) and SnO_2 (JCPDS file No. 46-1088), respectively. The characteristic sharp peaks could be indexed to the crystal faces with (002), (102), and (004) at 34.4, 47.5, and 72.6. In addition, the patterns have distinct diffraction peaks at 26.5, 37.7, 51.7, 61.7, and 65.7, which could be indexed to the SnO_2 structure on the FTO. Due to the low content of CNQDs in the composite, the diffraction peaks of CNQDs cannot be clearly observed in these patterns. Final, the results show that the ZnO nanowire arrays were successfully synthesized and are good agreement with the SEM results.

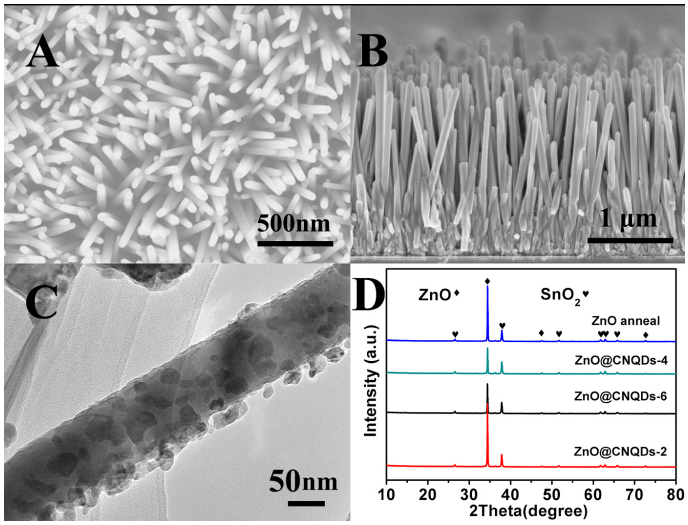

Figure 1. (**A**) SEM images of ZnO nanowire arrays. (**B**) SEM images of the horizontal cross section. (**C**) TEM images of ZnO@CNQDs. (**D**) XRD patterns of ZnO nanowire arrays, ZnO@CNQDs-2, ZnO@CNQDs-4, and ZnO@CNQDs-6.

With a view to further investigate, the energy-dispersive spectroscopy (EDS) results are exhibited as shown in Figure 2A, we can see that the O, Zn, C, and N elements are detected, which confirms the high purity of ZnO@CNQD composite products and the existence of CNQDs. Figure 2B–F show the linear sweep mapping results of the ZnO@CNQD composite electrodes. Zn, O, C, and N can be seen. More precisely, the location of C and N is in good agreement with the substance, as shown in Figure 2D. It demonstrates that the CNQDs were successfully loaded to the ZnO nanowires. As a result, it can be reasonably speculated that a portion of CNQDs was deposited onto the surface of ZnO nanowire arrays. This structure benefitted to the separation of photon-generated carriers and the improvement of photocurrent.

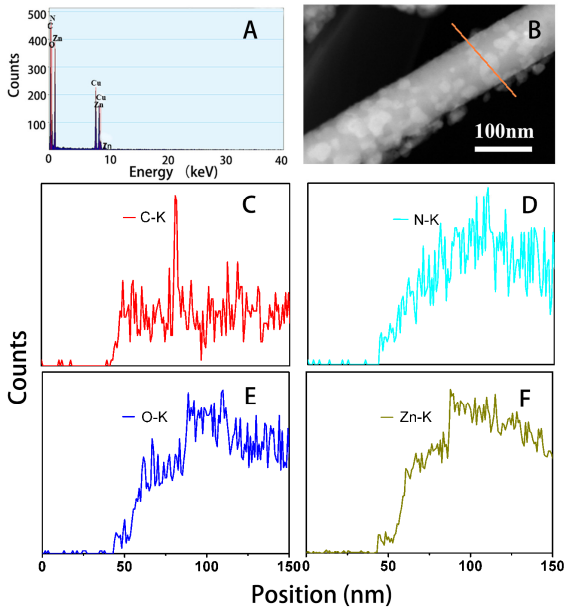

Figure 2. (**A**) EDX patterns of the ZnO@CNQD composite electrodes; (**B**–**F**) the linear sweep mapping results of the ZnO@CNQD composite electrodes.

In order to determine the chemical composition of ZnO@CNQDs-4 and identify the chemical state of the elements in the sample, X-ray photoelectron spectroscopy (XPS) spectra were employed, as shown in Figure 3A–D. We can see that all peaks in accordance with O, Zn, C, and N were clearly detected. The two sharp peaks at 1044.6 eV (Zn $2p_{1/2}$) and 1021.6 eV (Zn $2p_{3/2}$) are well matched with the reported values of ZnO, as shown in Figure 3A [32]. Figure 3B shows the O 1S core level centered at 531.6, in good agreement with the literature [33]. Figure 3C displays the C 1S XPS spectrum, two peaks in which can be distinguished to be centered at 284.6 eV and 288.2 eV, respectively. The peak at 284.6 eV is exclusively assigned to the adventitious hydrocarbon, and another one at 288.2 eV is identified as carbon atoms that have one double bond and two single bonds with three N neighbors [34,35]. The high-resolution spectrum of N 1S in ZnO@CNQDs suggests the coexistence of distinguishable models. A signal deconvolution after a Gaussian curve fitting is also displayed in Figure 2D, which revealed chemically different N species in the CNQDs with their N 1s binding energy at 398.7 eV and 400.1 eV, respectively. The N 1S binding energy of 398.7 eV can be assigned to Sp2-hybridized nitrogen (C=N–C) [17]. The binding energy of 400.1 eV may be attributed to tertiary nitrogen (N–$(C)_3$). The N–$(C)_3$ group confirmed the polymerization of melamine [36]. The results of XPS proved the CNQDs successful growth on the surface of ZnO nanowire arrays.

Figure 4 gives the UV-Vis light absorption spectra of the CNQD-modified ZnO nanowire arrays and the pure ZnO nanowire arrays. An absorption edge of the original ZnO at about 380 nm can be seen, and it has varying degrees of red shift after CNQDs are added. It can be inferred that these new nanoparticles could be more efficiently employed to the utilization of solar power.

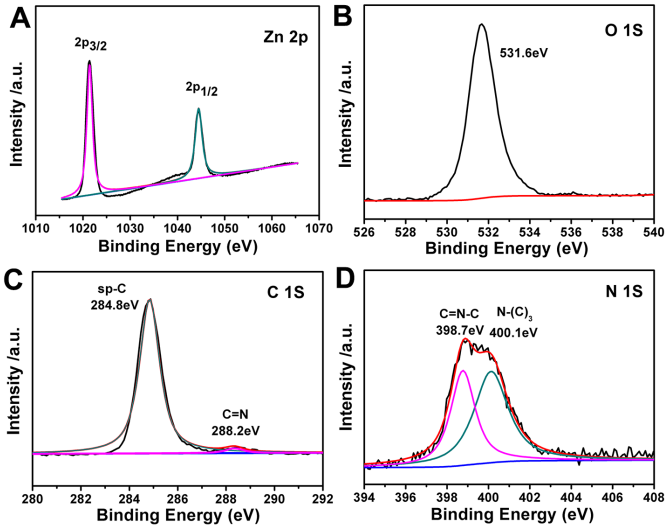

Figure 3. XPS spectra of ZnO@CNQDs-4: (**A**) Zn 2p; (**B**) O 1S; (**C**) C 1S; (**D**) N 1S.

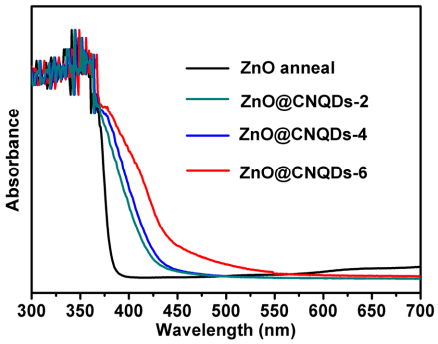

Figure 4. The UV diffuses reflectance spectra of ZnO, ZnO@CNQDs-2, ZnO@CNQDs-4, and ZnO@CNQDs-6.

2.2. PEC Performance

We investigated the photoelectrochemical properties of the ZnO@CNQD composite electrodes with simulated solar irradiation. More specifically, an experiment was carried out in 0.2 M Na_2SO_4 solution under illumination of 100 mW/cm^2 coupled with an AM 1.5 filter to supply simulated solar irradiation, and linear-sweep voltammograms under transient illumination are presented in Figure 5A. It can be seen that the composite electrodes have a very low photocurrent onset potential than that of pure ZnO, which demonstrates that the composites electron–hole separation is more outstanding under simulated solar irradiation. Figure 5B shows that the ZnO@CNQDs-4 composites with a certain content of CNQD-loaded electrodes have the highest photocurrent density (3.8 mA/cm^2) (0.6 V vs. SCE). As a result, fivefold enhanced photoelectrochemical performances of this novel hierarchical hetero-array compared with the pure ZnO nanowire arrays were obtained. With decreases of the CNQDs loaded, the photoelectrochemical properties also decreased. On the basis of the above results, the photocurrent properties of ZnO are remarkably enhanced with the CNQDs loaded. This was attributed to the charge transfer between CNQDs and ZnO nanowire arrays. Zhang et al. synthesized $ZnFe_2O_4$-modified CdS quantum dot/ZnO nanorod core/shell structured photoanodes, which showed the highest current density of 3.88 mA/cm^2 at 0 V (vs. Ag/AgCl) [32]. In addition, several other studies have shown that ZnO can be modified to show a high photocurrent [37–39].

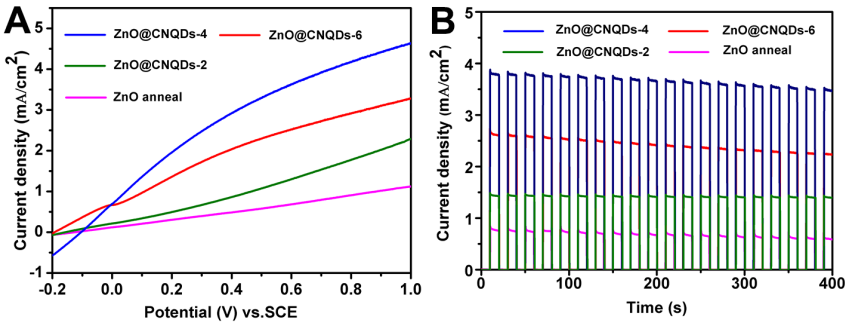

Figure 5. (**A**) Linear sweep voltammograms of ZnO nanowire arrays, ZnO@CNQDs-2, ZnO@CNQDs-4 and ZnO@CNQDs-6. (**B**) Amperometric *I*–*t* curves of ZnO nanowire arrays, ZnO@CNQDs-2, ZnO@CNQDs-4, and ZnO@CNQDs-6.

The electrochemical impedance spectroscopy (EIS) is an effective means to probe the interfacial charge transfer on the electrode. Here, the interfacial charge transfer resistance (*R*ct) can indicate by the semicircle diameter in a Nyquist plot. Figure 6 showed that the samples exhibited much lower *R*ct under illumination (Figure 6A) compared to no light (Figure 6B), which suggested the fast interfacial charge transfer under light illumination. It is necessary to note that the ZnO@CNQDs-4 electrode revealed the lowest *R*ct, which proves the faster separation of photogenerated charges. The remarkable charge separation between CNQDs and ZnO nanowire arrays were obtained, and this effect was assigned to the synergetic effect of the two substances. The diameter of all composite samples were smaller than the original ZnO, illustrating that the use of CNQDs promotes the process of charge transfer. In addition, the smaller *R*ct of ZnO@CNQDs-4 than that of the others proves that component concentration plays an important role in promoting charge separation and transfer. Therefore, the particular structure of CNQDs/ZnO composites contributed to the separation of photon-generation carriers and enhance photoelectric current.

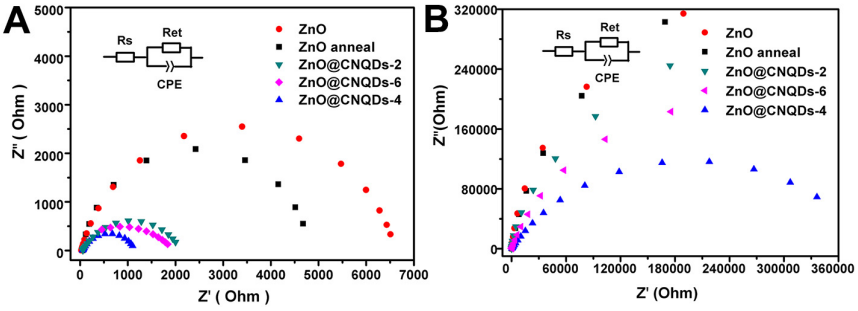

Figure 6. Electrochemical impedance spectroscopy (EIS) Nyquist plots of ZnO nanowire arrays, ZnO@CNQDs-2, ZnO@CNQDs-4, and ZnO@CNQDs-6: (**A**) light; (**B**) dark.

The incident photon-to-current conversion efficiency (IPCE) of ZnO@CNQDs and ZnO were used and are shown in Figure 7. IPCE was calculated as follows:

$$\mathrm{IPCE}(\%) = \frac{1240 \times I\left(\mathrm{mA/cm^2}\right)}{P_{\mathrm{Light}\left(\frac{\mathrm{mW}}{\mathrm{cm^2}}\right)} \times \lambda(\mathrm{nm})} \times 100$$

Here, the λ is the wavelength of incident light, I is the measured photocurrent density at a specific wavelength, and P_{light} is the measured light power density at that wavelength. The incident photon-to-current conversion efficiency (IPCE) analysis of ZnO@CNQDs showed that the ZnO@CNQDs reached a maximum of 96.8% at 370 nm (the photocurrent density is 0.997 $\mathrm{mA/cm^2}$ and measured light power density is 3.45 $\mathrm{mW/cm^2}$), while the ZnO nanowire arrays achieve 28.8% at this wavelength (the photocurrent density is 0.297 $\mathrm{mA/cm^2}$ and measured light power density is 3.45 $\mathrm{mW/cm^2}$).

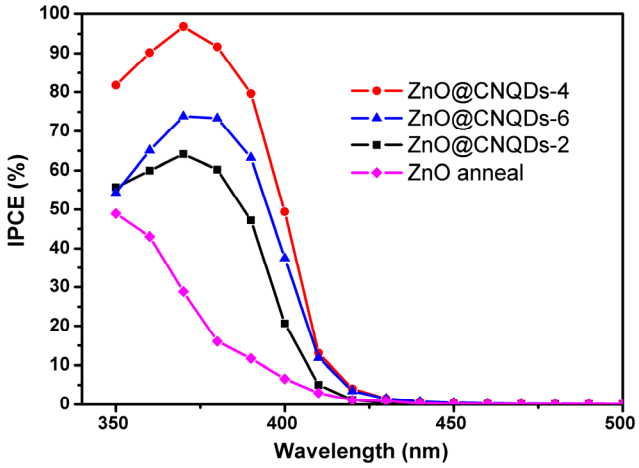

Figure 7. The incident photon-to-current conversion efficiency (IPCE) of ZnO nanowire arrays, ZnO@CNQDs-2, ZnO@CNQDs-4, and ZnO@CNQDs-6.

2.3. Photocatalytic Hydrogen Production

Figure 8 exhibits the photoelectrochemistry hydrogen evolution from splitting water using simulated solar irradiation. In this experiment, the H_2 was generated from the Pt counter electrode and was detected with gas chromatography (GC). It was detected that the maximum amount of H_2 generated on the ZnO@CNQDs-4 photocatalyst was 14 μmol with in 70 min. Simultaneously, the pure ZnO only produce trace amounts of H_2 (5 μmol after 70 min) under the same conditions, which indicated the low photogenerated electrons in the pure ZnO electrode compared with that of the

ZnO@CNQD composite electrodes. It exhibited that the ZnO@CNQD composite electrodes showed better photoelectrochemical phenomena as well as H_2 generation rates compared with the primary ZnO nanowire arrays. This confirmed that the CNQDs promoted the photoelectrochemical activities of the ZnO nanowire arrays.

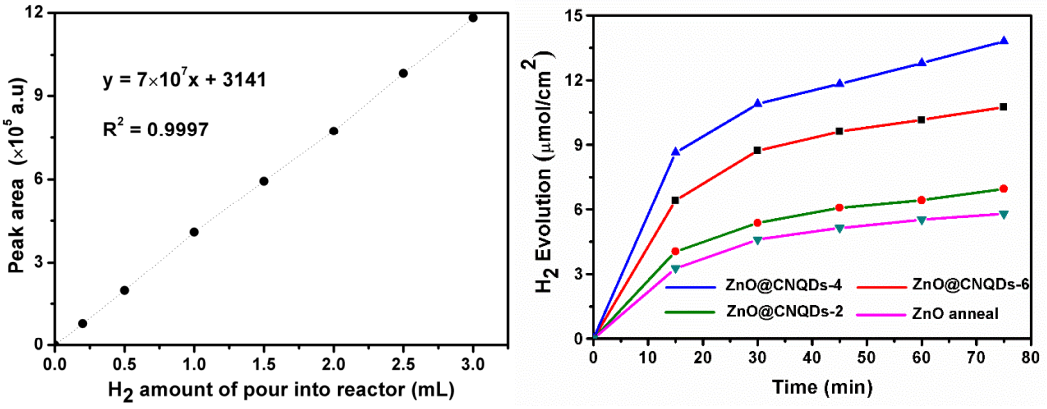

Figure 8. Photoelectrochemistry hydrogen evolution patter of ZnO nanowire arrays, ZnO@CNQDs-2, ZnO@CNQDs-4, and ZnO@CNQDs-6.

2.4. Mechanism of the Photoelectrochemistry Hydrogen Evolution

Based on the above results, the possible mechanism of photoelectrochemistry hydrogen evolution over the CNQDs/ZnO composite electrodes can be explained with Scheme 1 [40,41]. Under simulated sunlight irradiation, the electronic photons are excited from the valence band of ZnO to the conduction band and leave a hole on the valence band. Where CNDQs act as a solid-state electronic transfer reagent to trap photo-induced electrons, the photogenerated electrons on ZnO can be more efficiently transferred with the aid of CNDQs and efficient recombination with the hole. Then, the electron trap with CNDOs quickly transferred to the Pt plate by chemical workstation exerts a positive bias. Here, the electrons on the Pt plate combined with H^+ come from the electrolyte for generation hydrogen. Meanwhile, the hole of the valence band can be reacted with sulfite to form sulfate.

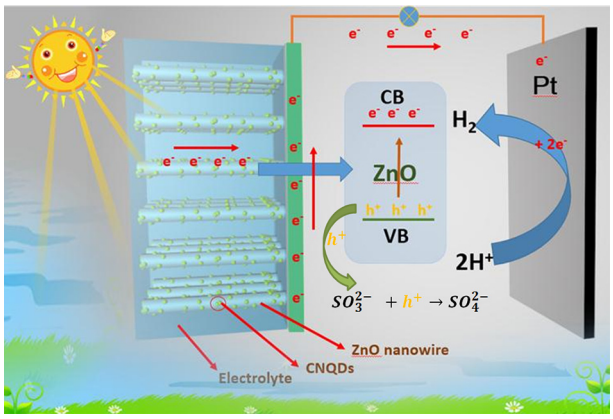

Scheme 1. Schematic of photoelectrochemistry hydrogen evolution over the CNODs/ZnO composite electrodes.

3. Materials and Methods

3.1. Catalyst Preparation

3.1.1. g-C_3N_4 Quantum Dots (CNQDs) Preparation

Graphite-like carbon nitride quantum dots were prepared as follows: heating thiourea (Aldrich, St. Louis, MO, USA, 99%) at 550 °C for 2 h to obtain a bulk g-C_3N_4. A certain amount of g-C_3N_4 were put on an open ceramic container, followed by a thermal treatment process at a temperature of 500 °C for 2 h (ramp rate of 2 °C/min) to obtain g-C_3N_4 nanosheets. Then, 0.05 g g-C_3N_4 nanosheets were handled in concentrated H_2SO_4 (10 mL) and HNO_3 (30 mL) for 16 h under ultrasonication (500 W, 40 kHz). The obtained clear solution was then diluted with deionized (DI) water (200 mL) to produce a colloidal suspension, and then centrifuged to remove the acids. The suspended matter was transferred into a poly tetrafluoroethylene autoclave (20 mL) and heated at 200 °C for 10 h. Then, we cooled it to room temperature, the final product of the yellowish CNQDs solution (~0.14 g/L) was filtered through a 0.22 μm microporous membrane, and the CNQDs were obtained.

3.1.2. ZnO Nanowire Arrays Preparation

In a typical procedure, at first, prepared 1.0 M ZnO sol as follows: 24 mmol zinc acetate dehydrate [$Zn(CH_3COO)_2{\cdot}2H_2O$] was dissolved in 20 mL ethylene glycol monomethyl [CH_3O-CH_2-CH_2OH], and then diethanolamine (DEA) with an equal mole was add in. Then, the above sol coated on an FTO glasses substrate ($10 \times 50 \times 1$ mm^3) with a VTC-100vacuum spin coater followed with a calaination of 150 °C for 15 min and repeated it 3 times. Then, the prepared FTO was calcined under 350 °C for 30 min to get the ZnO seed layer. This ZnO seed layer was transferred into a 100 mL tetrafluoroethylene autoclave, which contained 0.04 M $Zn(NO_3)_2{\cdot}6H_2O$ and 0.04 M hexamethylenetetramine (HMT) for growing ZnO at 95 °C maintain 9 h. Subsequently, the autoclave was cooled down to the room temperature and the obtained ZnO nanowire arrays were washed with deionized water and ethanol several times in order to remove the ionic residual and dried at 60 °C for 30 min.

3.1.3. ZnO@CNQD Composites Electrode Preparation

Composite electrodes were prepared by the coating drop method. The specific approach is as follows: 100 μL of CNQDs is coated on the as-synthesized ZnO nanowire arrays by means of one coating drop per round and heated to 150 °C until dry. This round is repeated 2, 4, and 6 times in order to prepare three composite electrodes, respectively. Then, these composite electrodes are annealed for 2.5 h with 500 °C (ramp rate of 2 °C/min).

3.2. Characterization

A field emission scanning electron microscope (JEOL-JSM6701F, Tokyo, Japan) was employed to observe the morphology and structure of the samples at an accelerating voltage of 5 kV. X-ray diffraction analysis (XRD, Rigaku RINT-2000, Rigaku, Tokyo, Japan) with Cu Kα radiation at 40 k eV and 40 mA was used to identify the crystalline structure of the products. X-ray photoelectron spectroscope (XPS, ESCALAB 250 Xi, Thermo Fisher Scientific, MA, USA) was employed to detect element composition. Transmission electron microscopy (TEM) and high-resolution TEM (HRTEM) images were taken with a Tecnai-G2-F30 field emission transmission electron microscope operating at an accelerating voltage of 300 kV(FEI, Hillsboro, AL, USA). UV-visible diffuse reflectance spectra were taken on a UV-2550 (Shimadzu, Tokyo, Japan) spectrometer.

3.3. PEC Measurements and Photoelectric Hydrogen Production

All photoelectrochemical performances were conducted in a three-electrode system. Specifically, a saturated calomel electrode (SCE) was employed as a reference electrode, with a piece of Pt foil (3×2 cm^2) as a counter electrode. The ZnO nanowire arrays and the ZnO@CNQD composite

electrodes were used as the working electrodes (an available surface area of 1 cm^2). A 0.2 M Na_2SO_4 aqueous solution was applied as the electrolyte (with pH buffered to 7.0). The electrochemical measurements were tested using a CHI760D electrochemical workstation.

All photoelectrodes were illuminated from the front a 300 W Xe lamp (HSX-F/UV 300) equipped with a 1.5 cutoff filter (HSX-F300, Beijing NBeT Technology Co., Ltd., Beijing, China) calibrated to 100 mW/cm^2. Linear sweep voltammograms were measured under a bias voltage between −0.2 V and 1.0 V (vs. SCE) with a scan rate of 0.1 V/s. Amperometric *I–t* curves were tested at a bias voltage of +0.6 V (vs. SCE). The incident photon to current efficiency (IPCE) was measured using a full solar simulator (Model 9600, 300 W Xe arc lamp, Newport, New York, NY, USA) and a motorized monochromator (Oriel Cornerstone 130 1/8 m). IPCE was measured at 0.7 V vs. SCE in 0.5 M Na_2SO_4 (pH = 7) using the same three-electrode setup described above for the photocurrent measurements. The electrochemical impedance spectroscopy (EIS) measurements were carried out via the CHI-760D workstation in a three-electrode cell by applying an AC voltage with a 5 mV amplitude in a frequency range from 1 Hz to 100 kHz under open circuit potential conditions.

Photoelectrochemical H_2 evolution was studied via applied 0.6 V voltage bias vs. SCE and 0.5 M phosphate with pH = 7 used as a buffer in 1 M Na_2SO_3 electrolyte. Here, Na_2SO_3 electrolyte acted as a photogenerated-hole scavenger, a saturated calomel electrode was used as a reference electrode, and a sample film and Pt plate were used as photoanodes and photocathodes, respectively. The opening of the cell was sealed with a silicone rubber septum.

In typical photocatalytic H_2 evolution experiments, the reactant mixture was degassed by bubbling N_2 gas for 40 min, and then was irradiated by a 300 W Xe lamp with a cutoff filter of 420 nm for H_2 evolution. An amount of H_2 generated from the Pt plate photocathodes was measured using gas chromatography (Tianmei GC7900, TCD, 13× column, N_2 as carrier, Tianmei, Shanghai, China). From the reactor, 0.5 mL of gas was extracted every 15 min to analyze the amount of H_2 generated by using gas chromatography.

4. Conclusions

In summary, we exhibited a toilless coating process for manufacturing CNQDs/ZnO composite electrodes. The remarkably quantum confinement properties of CNQDs was carefully studied by means of SEM, EDS, XPS, UV-VIS diffuse reflectance, PEC performance, photoelectric hydrogen production, etc., and the results are in good agreement. With the decoration of CNQDs, the photoelectrochemical performances of the composite electrodes were greatly enhanced, and the quantum confinement effect of CNQDs was achieved. This "Herpes-Rods" structure of CNQDs/ZnO composite is contributed to the separation of photon-generated carriers and to enhance photoelectric current. CNQDs/ZnO can produce H_2 approximately 5 times five fold higher than that of the pure ZnO electrode under solar simulating irradiation. Here, the CNQDs/ZnO composite electrodes exhibited better photoelectrochemical properties as well as hydrogen generation rates compared with the primary ZnO nanowire arrays, and confirmed that the CNQDs actually promote the photoelectrochemical performances of original ZnO as well. Further studies showed that the absorption edge of CNQD-modified ZnO nanowire arrays is slightly broadened, and the diameter of *R*ct was smaller than that of the primary ZnO. The assembly of CNQDs promoted the charge transfer process. The smaller *R*ct of CNQDs-4/ZnO compared to those of others implies that the component concentration played an important role in enhancing charge separation and transfer. Because ZnO nanowire arrays have high electron mobility and a low onset potential due to their linear structure, the introduction of CNQDs to further enhance the photocurrent properties of ZnO. A possible mechanism of photoelectrochemistry hydrogen evolution over CNQDs/ZnO composite electrodes is thus proposed. This work provides a possible strategy towards the development of sustainable clean energy. This strategy may be applied to construct other ZnO nanowire arrays based on the quantum confinement effect of CNQDs for solar photoelectric conversion.

Acknowledgments: This work was financially supported by the Chinese National Natural Science Foundation (21603274, 41663012, 21263001 and 21463001).

Author Contributions: Hao Yang and Zhiliang Jin conceived and designed the experiments; Hao Yang performed the experiments; Yingpu Bi and Gongxuan Lu contributed reagents and analysis tools; Hongyan Hu and Hao Yang analyzed the date; Hao Yang wrote the paper.

Conflicts of Interest: The authors declare no conflict of interest.

References

1. Harvey, B.G.; Merriman, W.W.; Koontz, T.A. High-Density Renewable Diesel and Jet Fuels Prepared from Multi cyclic Sesqui terpanes and a 1-Hexene-Derived Synthetic Paraffinic Kerosene. *Energy Fuels* **2015**, *29*, 2431–2436. [CrossRef]
2. Walter, M.G.; Warren, E.L.; McKone, J.R.; Boettcher, S.W.; Mi, Q.; Santori, E.A.; Lewis, N. S. Solar Water Splitting Cells. *Chem. Rev.* **2010**, *110*, 6446–6473. [CrossRef] [PubMed]
3. Bak, T.; Nowotny, J.; Rekas, M.; Sorrell, C.C. Photo-electrochemical hydrogen generation from water using solar energy. Materials-related aspects. *Int. J. Hydrogen Energy* **2002**, *27*, 991–1022. [CrossRef]
4. Hisatomi, T.; Kubota, J.; Domen, K. Recent advances in semiconductors for photocatalytic and photoelectrochemical water splitting. *Chem. Soc. Rev.* **2014**, *43*, 7520–7535. [CrossRef] [PubMed]
5. Tran, P.D.; Wong, L.H.; Barber, J.; Loo, S.C. Recent advances in hybrid photocatalysts for solar fuel production. *Energy Environ. Sci.* **2012**, *5*, 5902–5918. [CrossRef]
6. Chen, X.; Shen, S.; Guo, L.; Mao, S.S. Semiconductor-based photocatalytic hydrogen generation. *Chem. Rev.* **2010**, *110*, 6503–6570. [CrossRef] [PubMed]
7. Pinna, N.; Neri, G.; Antoniett, M.; Niederberger, M. Nonaqueous synthesis of nanocrystalline semiconducting metal oxides for gas sensing. *Angew. Chem. Int. Ed.* **2004**, *116*, 4445–4449. [CrossRef]
8. Shankar, K.; Mor, G.K.; Prakasam, H.E.; Yoriya, S.; Paulose, M.; Varghese, O.K.; Grimes, C. Highly-ordered TiO_2 nanotube arrays up to 220 μm in length: use in water photoelectrolysis and dye-sensitized solar cells. *Nanotechnology* **2007**, *18*, 065707. [CrossRef]
9. Zheng, J.Y.; Son, S.I.; Van, K.T.; Kang, Y.S. Preparation of α-Fe_2O_3 films by electrodeposition and photodeposition of Co-Pi on them to enhance their photoelectrochemical properties. *RSC Adv.* **2015**, *5*, 36307–36314. [CrossRef]
10. Zhang, H.; Liu, F.; Mou, Z.; Liu, X.; Sun, J.; Lei, W. A facile one-step synthesis of ZnO quantum dots modified poly (triazine imide) nanosheets for enhanced hydrogen evolution under visible light. *Chem. Commun.* **2016**, *52*, 13020–13023. [CrossRef] [PubMed]
11. Pawar, A.U.; Kim, C.W.; Kang, M.J.; Kang, Y.S. Facile Fabrication of WO_3 Nanoplates Thin Films with Dominant Crystal Facet of (002) for Water Splitting. *Nano Energy* **2016**, *20*, 156–167. [CrossRef]
12. Zhang, J.Z. Metal oxide nanomaterials for solar hydrogen generation from photoelectrochemical water splitting. *MRS Bull* **2011**, *36*, 48–55. [CrossRef]
13. Wang, T.; Jin, B.; Jiao, Z.; Lu, G.; Ye, J.; Bi, Y. Photo-directed growth of Au nanowires on ZnO arrays for enhancing photoelectrochemical performances. *J. Mater. Chem. A* **2014**, *2*, 15553–15559. [CrossRef]
14. Mclaren, A.; Valdes-Solis, T.; Li, G.; Tsang, S.C. Shape and size effects of ZnO nanocrystals on photocatalytic activity. *J. Am. Chem. Soc.* **2009**, *131*, 12540–12541. [CrossRef] [PubMed]
15. Cho, S.; Jang, J.; Kim, J.; Lee, J.; Choi, W.; Lee, K. Three-Dimensional Type II ZnO/ZnSe Heterostructures and Their Visible Light Photocatalytic Activities. *Langmuir* **2011**, *27*, 10243–10250. [CrossRef] [PubMed]
16. Wang, T.; Jin, B.; Jiao, Z.; Lu, G.; Ye, J.; Bi, Y. Electric field-directed growth and photoelectrochemical properties of cross-linked Au-ZnO hetero-nanowire arrays. *Chem. Commun.* **2015**, *51*, 2103–2106. [CrossRef] [PubMed]
17. Ai, G.; Li, H.; Liu, S.; Mo, R.; Zhong, J. Solar Water Splitting by TiO_2/CdS/Co–Pi Nanowire Array Photoanode Enhanced with Co–Pi as Hole Transfer Relay and CdS as Light Absorber. *Adv. Funct. Mater.* **2015**, *25*, 5706–5713. [CrossRef]
18. Guo, C.X.; Xie, J.; Yang, H.; Li, C.M. Au@CdS Core–Shell Nanoparticles-Modified ZnO Nanowires Photoanode for Efficient Photoelectrochemical Water Splitting. *Adv. Sci.* **2015**, *2*, 2084–2088. [CrossRef] [PubMed]

19. Jin, B.; Jiao, Z.; Bi, Y. Efficient Charge Separation between Bi_2MoO_6 Nanosheets and ZnO Nanowires for Enhanced Photoelectrochemical Properties. *J. Mater. Chem. A* **2015**, *3*, 19702–19705. [CrossRef]
20. Hao, X.Q.; Jin, Z.L.; Min, S.X.; Lu, G.X. Modulating photogenerated electron transfer with selectively exposed Co–Mo facets on a novel amorphous g-C_3N_4/$Co_xMo_{1-x}S_2$ photocatalyst. *RSC Adv.* **2016**, *6*, 23709–23717. [CrossRef]
21. Hao, X.Q.; Jin, Z.L.; Lu, G.X. Enhanced Surface Electron Transfer with the Aid of Methyl Viologen on the Co_3O_4-g-C_3N_4 Photocatalyst. *Chem. Lett.* **2016**, *45*, 116–118. [CrossRef]
22. Li, C.; Wang, Z.; Sui, X.; Zhang, L.; Gu, D. Graphitic-C_3N_4 quantum dots modified carbon nanotubes as novel support material for low Pt loading fuel cell catalyst. *RSC Adv.* **2016**, *6*, 32290–32297. [CrossRef]
23. Li, G.; Lian, Z.; Wang, W.; Zhang, D.; Li, H. Nanotube-confinement induced size-controllable g-C_3N_4 quantum dots modified single-crystalline TiO_2 nanotube arrays for stable synergetic photoelectrocatalysis. *Nano Energy* **2016**, *19*, 446–454. [CrossRef]
24. Pan, D.; Xi, C.; Li, Z.; Wang, L.; Chen, Z.; Lu, B.; Wu, M. Electrophoretic fabrication of highly robust, efficient, and benign hetero junction photoelectrocatalysts based on graphene-quantum-dot sensitized TiO_2 nanotube arrays. *J. Mater. Chem. A* **2013**, *1*, 3551–3555. [CrossRef]
25. Hao, X.Q.; Jin, Z.L.; Xu, J.; Min, S.X.; Lu, G.X. Functionalization of TiO_2 with graphene quantum dots for efficient photocatalytic hydrogen evolution. *Superlattices Microstruct.* **2016**, *94*, 237–244. [CrossRef]
26. Hao, X.Q.; Yang, H.; Jin, Z.L.; Xu, J.; Min, S.X.; Lu, G.X. Quantum confinement effect of graphene-like C_3N_4 nanosheets for efficient photocatalytic hydrogen production from water splitting. *Acta Phys. Chim. Sin.* **2016**, *32*, 2581–2592.
27. Zhuo, S.; Shao, M.; Lee, S. Comment on "Upconversion and downconversion fluorescent graphene quantum dots: ultrasonic preparation and photocatalysis". *ACS Nano* **2012**, *6*, 1059–1064. [CrossRef] [PubMed]
28. Ma, Y.; Li, X.; Yang, Z.; Xu, S.; Zhang, W.; Su, Y.; Hu, N.; Lu, W.; Feng, J.; Zhang, Y. Morphology control and photocatalysis enhancement by in-situ hybridization of Cu_2O with nitrogen-doped carbon quantum dots. *Langmuir* **2016**, *32*, 9418–9427. [CrossRef] [PubMed]
29. Su, J.; Zhu, L.; Chen, G. Ultrasmall graphitic carbon nitride quantum dots decorated self-organized TiO_2, nanotube arrays with highly efficient photoelectrochemical activity. *Appl. Catal. B Environ.* **2016**, *186*, 127–135. [CrossRef]
30. Niu, P.; Zhang, L.; Liu, G.; Cheng, H. Graphene-Like Carbon Nitride Nanosheets for Improved Photocatalytic Activities. *Adv. Funct. Mater.* **2012**, *22*, 4763–4770. [CrossRef]
31. Wang, W.; Yu, J.C.; Xia, D.; Wong, P.K.; Li, Y. Graphene and g-C_3N_4 nanosheets cowrapped elemental α-sulfur as a novel metal-free heterojunction photocatalyst for bacterial inactivation under visible-light. *Environ. Sci. Technol.* **2013**, *47*, 8724–8732. [CrossRef] [PubMed]
32. Cao, S.; Yan, X.; Kang, Z.; Liang, Q.; Liao, X.; Zhang, Y. Band alignment engineering for improved performance and stability of $ZnFe_2O_4$, modified CdS/ZnO nanostructured photoanode for PEC water splitting. *Nano Energy.* **2016**, *24*, 25–31. [CrossRef]
33. Vijayan, T.A.; Chandramohan, R.; Valanarasu, S.; Thirumalai, J.; Venkateswaran, S.; Mahalingam, T.; Srikumar, S.R. Optimization of growth conditions of ZnO nano thin films by chemical double dip technique. *Sci. Technol. Adv. Mater.* **2008**, *9*, 035007. [CrossRef] [PubMed]
34. Yan, S.C.; Li, Z.S.; Zou, Z.G. Photodegradation performance of g-C_3N_4 fabricated by directly heating melamine. *Langmuir* **2009**, *25*, 10397–10410. [CrossRef] [PubMed]
35. Liu, L.; Ma, D.; Zheng, H.; Li, X.; Cheng, M.; Bao, X. Fe-doped and -mediated graphitic carbon nitride nanosheets for enhanced photocatalytic performance under natural sunlight. *Microporous Mesoporous Mater.* **2008**, *110*, 216–222. [CrossRef]
36. Thomas, A.; Fischer, A.; Goettmann, F.; Antonietti, M.; Müller, J.; Schlöglb, R.; Carlsson, J.M. ChemInform Abstract: Graphitic Carbon Nitride Materials: Variation of Structure and Morphology and Their Use as Metal-Free Catalysts. *J. Mater. Chem.* **2008**, *18*, 4893–4908. [CrossRef]
37. Choi, Y.; Baek, M.; Zhang, Z.; Dao, V.D.; Choi, H.S.; Yong, K. A two-storey structured photoanode of a 3D Cu_2ZnSnS_4/CdS/ZnO@ steel composite nanostructure for efficient photoelectrochemical hydrogen generation. *Nanoscale* **2015**, *7*, 15291–15299. [CrossRef] [PubMed]
38. Cheng, C.; Zhang, H.; Ren, W.; Dong, W.; Sun, Y. Three dimensional urchin-like ordered hollow TiO_2/ZnO nanorods structure as efficient photoelectrochemical anode. *Nano Energy* **2013**, *2*, 779–786. [CrossRef]

39. Wang, G.; Yang, X.; Qian, F.; Zhang, J.Z.; Li, Y. Double-Sided CdS and CdSe Quantum Dot Co-Sensitized ZnO Nanowire Arrays for Photoelectrochemical Hydrogen Generation. *Nano Lett.* **2010**, *10*, 1088–1092. [CrossRef] [PubMed]
40. Cha, H.G.; Kang, M.J.; Hwang, I.C.; Kim, H.; Yoon, K.B.; Kang, Y.S. Manual assembly of nanocrystals for enhanced photoelectrochemical efficiency of hematite film. *Chem. Commun.* **2015**, *51*, 6407–6410. [CrossRef] [PubMed]
41. Van, T.K.; Pham, L.Q.; Kim, D.Y.; Zheng, J.Y.; Kim, D.; Pawar, A.U.; Kang, Y.S. Facile Fabrication of WO_3 Nanoplates Thin Films with Dominant Crystal Facet of (002) for Water Splitting. *Chemsuschem* **2014**, *7*, 3505–3512. [CrossRef] [PubMed]